JOURNAL OF MATERIALS SCIENCE 32 (1997) 737–740

Comparative study of measured attenuation with the Rayleigh region scattering theory

S. MUKHERJEE, A. K. DE, K. K. PHANI
Central Glass and Ceramic Research Institute, Calcutta 700 032, India

The study of ultrasonic attenuation by a non-destructive method has an important role in characterizing the mechanical behaviour of different types of materials. The values of sound absorption coefficient (attenuation) of sintered magnesium aluminosilicate glass powder at different frequencies have been measured by the pulse echo method and the data were fitted considering Rayleigh region scattering. Because the sample consists of two phases, one glass and the other ceramic (cordierite), the value of the scattering coefficient can be calculated from the theory by considering a two-phase medium and this value can be compared with that from the Rayleigh region scattering part. The two values of the scattering coefficient are in fair agreement.

1. Introduction

Ultrasonic scattering is an important technique for non-destructive evaluation of materials such as plastics, metals, composites and ceramics. When an elastic wave propagates through a medium, it is quite logical to assume that the nature of the propagation of the wave differs depending upon the nature of the medium. Scattering of the waves takes place and this scattering is fully dependent upon the inhomogeneities inherent in the medium. Because the inhomogeneities of different samples are not same, the characterization of the samples can be done by studying the scattering of the elastic waves and thus the scattering properties may be regarded as the basis of such a classification.

Microstructural evaluation of metals have already been done by many researchers [1–4] using the ultrasonic scattering properties as a tool. This technique has been extensively used for the evaluation of microstructures of polycrystalline materials during the last two decades [1, 5]. Ultrasonic attenuation is a suitable parameter to use to evaluate the microstructural configuration of polycrystalline materials and hence a quantitative knowledge of ultrasonic attenuation in materials gives an idea about the microstructure such as grain size, pore size, pore concentration, etc. [6, 7]. The effect of scattering of high-frequency waves (both shear and longitudinal) due to grains in polycrystalline materials are not simple. The effective elastic constants differ from grain to grain. This difference occurs not only due to random orientation of the grains but also for different grain sizes. When the wave length is very large compared to grain size, Rayleigh scattering occurs and the attenuation is given by [8]

$$\alpha = af + bf^4 \quad (1)$$

where α is the attenuation coefficient, f is the frequency of the elastic wave, a is the elastic hysteresis coefficient, and b is the Rayleigh scattering coefficient. Equation 1 has been extensively used to compare the experimental values of attenuation of metallic systems [1–4, 9, 10]. The scattering phenomena have also been explained by theories based on polycrystalline systems [11–16] where the materials have grains of randomly distributed grain size. Evans *et al.* [17] have calculated the attenuation in a polycrystalline ceramic system on the assumption that the attenuation is dominated by the large extreme of microstructure.

In the present work, attenuation was measured and compared with the theoretical values which can be calculated by considering the distribution of the grain size measured from photomicrographs of the sintered magnesium aluminosilicate glass ceramic samples.

2. Experimental procedure

2.1. Sample preparation

Magnesium aluminosilicate glass powders were prepared from laboratory-made glass frit having the composition 25% Al_2O_3, 55% SiO_2 and 20% MgO. Discs, 25 mm diameter and 5 mm thick, were prepared by hydrostatic pressing at a pressure of $\sim$120 MPa; 5% PVA solution was used as a binder. The specimens were subjected to a thermal treatment initially at about 400 °C, to drive off PVA, and finally at about 950 °C in air. The rate of temperature rise was 150 °C h^{-1} with 1 h soaking at 950 °C. The sintered samples were ground and polished and finished to 1 μm. The faces were maintained parallel to within 0.002 mm.

2.2. Grain-size determination

The polished samples were etched chemically using 5% hydrofluoric acid. Photographs of the sample at different places on the surface were taken using

0022–2461

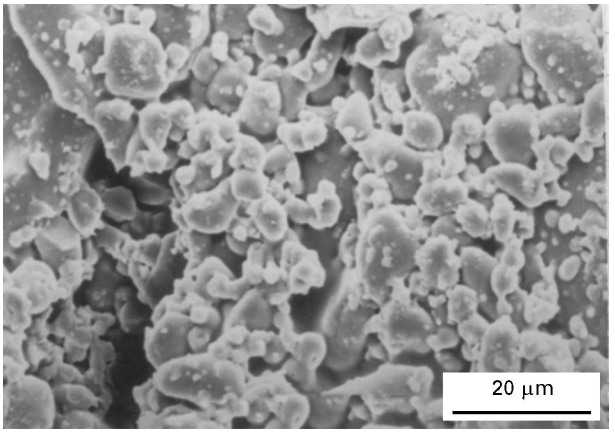

Figure 1 Photomicrograph of a sintered sample showing the grains.

standard metallographic techniques. A typical photomicrograph is shown in Fig. 1. The grain diameter distributions from these planar sections was evaluated by measuring the length of chords that corresponds to grain-boundary intersections at linear traces across the plane. The details of this calculation are given later.

2.3. Attenuation measurement

The ultrasonic attenuation measurements were made at room temperature by the ultrasonic pulse-echo method with a polystyrene buffer rod between the transducer and the sample. A Kraut Krammer ultrasonic tester USIP-12 and a 15 MHz broadband transducer (CLF4) were used for the measurement. The transducer emits longitudinal waves. The signals from the front surface reflection, A, first back surface reflection, B, and the front surface reflection without the sample, A', have been selected and digitized using a digitizing oscilloscope (Phillips model 3350) interfaced with the ultrasonic tester USIP-12 and stored in an IBM PC. Each digitized signal was Fourier transformed using an FFT algorithm after high-pass filtering above 6 MHz using a filtering algorithm. Attenuation coefficients, α, for different frequencies have been calculated by the A' AB method [18] using the equation

$$\alpha = \frac{1}{2l} \ln \left[\frac{A'(1 - R^2)}{B} \right] \tag{2}$$

where l and R are the thickness of the specimen and the reflection coefficient, respectively. R was calculated from [18]

$$R = -\frac{A}{A'} \tag{3}$$

It is well known that if the thickness of the couplant is very thin, then the reflection coefficient, R, is given by [19]

$$R = \frac{Z_S - Z_T}{Z_S + Z_T} \tag{4}$$

where Z_S and Z_T are the acoustic impedance of the specimen and the transducer, respectively. α values as

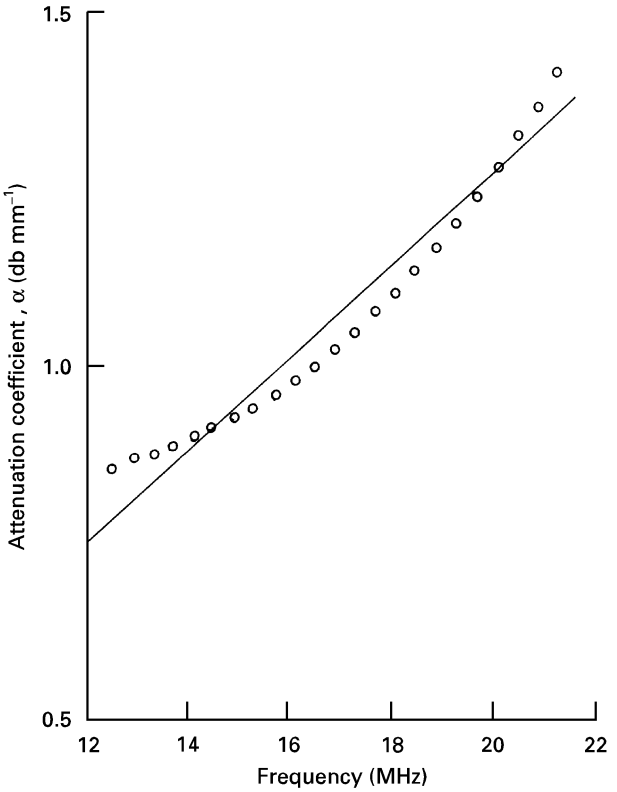

Figure 2 Variation of attenuation coefficient, α, with frequency; (○) experimental, (——) theoretical.

calculated from Equation 2 are limited to the range-bounded 1/10th of the peak amplitude of the frequency spectrum of signal B. Outside this range the calculation is subjected to large errors because of the low amplitude of the frequency components of the signal B [18]. The beam-diffraction corrections do not apply in the measurement.

3. Results and discussion

The experimental data of the attenuation measurements are shown in Fig. 2 and Equation 1 is fitted to the data by regression analysis. This gives

$$\alpha(\text{db mm}^{-1}) = 6.211 \times 10^{-2} f + 2.413 \times 10^{-7} f^4 \tag{5}$$

with a Q value of 0.952. Equation 5 is also plotted in Fig. 2, where Q is defined by

$$Q = 1 - \sum_{i=1}^{n} \left(\alpha_i - \hat{\alpha}_i \right)^2 \Big/ \sum_{i=1}^{n} \left(\alpha_i - \bar{\alpha}_i \right)^2 \tag{6}$$

where α_i is the measured value, $\hat{\alpha}_i$ is the calculated value from the fitted equation and $\bar{\alpha}_i$ is the mean of the measured value.

3.1. Theoretical prediction

3.1.1. A two-phase system

In this theoretical consideration, attenuation of the sound wave is dependent on the scattering cross-sections, Ω, of the predominant scatterers. The scattering cross-sections can be calculated from the solutions of both the scaler and vector potential with the boundary conditions that the stresses and displacements

vary continuously across the boundary of the embedded obstacle [13, 14]. In the Rayleigh region, the scattering cross-section is given by

$$\Omega = 4/9\ \pi g_e x_1^4 a^6 \tag{7}$$

where x_1 is the longitudinal wave number, a is the radius of the scatterer and, for an elastic spherical scatterer, g_e is given by [14]

$$g_e = \left\{\frac{3(k_1/x_1)^2}{[3(k_2/x_2)^2 - 4](\mu_2/\mu_1) + 4} - 1\right\}^2 + 1/3[1 + 2(k_1/x_1)^3][(k_2/k_1)^2(\mu_2/\mu_1) - 1]^2 + 40[2 + 3(k_1/x_1)^5] \times \left\{\frac{(\mu_2/\mu_1) - 1}{2[3(k_1/x_1)^2 + 2](\mu_2/\mu_1) + 9(k_1/x_1)^2 - 4}\right\}^2 \tag{8}$$

where x and k are the wave numbers for longitudinal and mode-converted transverse waves, respectively, and μ is the shear moduli. Subscripts 1 and 2 refer to matrix and scatterer, respectively. Assuming there is no interaction between individual scatterers, the attenuation is given by

$$\alpha = 1/2 \int_0^\infty n(D_i)\Omega(D_i, f)\,\mathrm{d}D_i \tag{9}$$

where Ω and D_i are the scattering cross-section and diameter of the ith scatterer, respectively, and $n(D_i)\mathrm{d}D_i$ is the number of scatterers per unit volume in the size range D_i to $D_i + \mathrm{d}D_i$, and is given by [20]

$$n(D) = \frac{2n(l)\mathrm{d}l}{\pi l^2} - \frac{2}{\pi l^2}\frac{\mathrm{d}n(l)}{\mathrm{d}l}\,\mathrm{d}l \tag{10}$$

where $n(l)\,\mathrm{d}l$ is the measured number of chords per unit length in the size range l to $l + \mathrm{d}l$. To evaluate $n(D)$ from Equation 10, the data on $n(l)$ versus l were analysed in terms of the Pearson probability density function [21], which gives a beta distribution of the form

$$n(D) = 1.025\,66 \times 10^{-11}(D - 3.908)^{1.1695} \times (14.367 - D)^{10.9257} \tag{11}$$

which is shown in Fig. 3. Using Equation 11, the total attenuation was evaluated from Equation 9 by numerical integration, which is given by

$$\alpha\,(\mathrm{db\,mm^{-1}}) = 2.851 \times 10^{-7} f^4 \tag{12}$$

where f is in MHz. From Equation 12, we obtain the value of the scattering coefficient calculated from scattering cross-section by considering the two-phase medium theory. This value of scattering coefficient is in fair agreement with that of the Rayleigh region scattering (coefficient of the second part of Equation 5). Therefore, it may be concluded that the attenuation measurement could be a powerful non-destructive technique for characterizing the microstructure of these types of sintered materials. In the above calculation we neglect the scattering due to small pores present in the material. But the agreement indicates that the pores do not contribute significantly to the scattering process at this level of porosity.

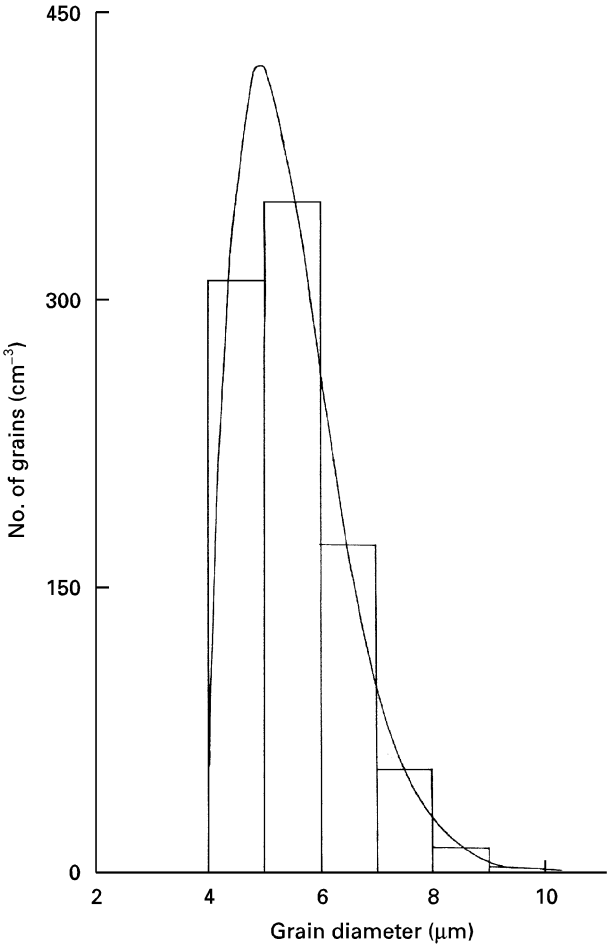

Figure 3 Distribution of the number of grains per unit volume with the grain diameter.

4. Conclusion

The attenuation in a sintered glass system was measured. The scattering coefficient was calculated from the two-phase medium theory. The experimental data were fitted to the Rayleigh region scattering and it was found that the scattering part of the fitted equation is in fair agreement with that calculated from the two-phase medium theory. This indicates that attenuation measurement could be a powerful approach for characterizing the microstructure of sintered materials.

Acknowledgement

The authors thank Dr B. K. Sarker, Director of the Central Glass and Ceramic Research Institute, for permission to publish this paper.

References

1. W. P. MASON and H. J. Mc-SKIMIN, *J. Appl. Phys.* **19** (1948) 940.
2. E. P. PAPADAKIS and E. L. REED, *ibid.* **32** (1961) 682.
3. R. N. LATIFF and N. F. FIORE, *ibid.* **45** (1974) 5182.
4. E. P. PAPADAKIS, *J. Acoust. Soc. Am.* **33** (1961) 1616.

5. W. ROTH, *J. Appl. Phys.* **19** (1948) 901.
6. D. K. HSU, D. O. THOMPSON and R. B. THOMPSON, *Rev. Progr. Quant. Non-Destruct. Eval.* **5B** (1986) 1633.
7. J. H. ROSE, *ibid.* **4B** (1985) 909.
8. W. P. MASON and H. J. Mc-SKIMIN, *J. Acoust. Soc. Am.* **19** (1947) 464.
9. E. P. PAPADAKIS, *J. Appl. Phys.* **34** (1965) 265.
10. E. P. PAPADAKIS, *J. Acoust. Soc. Am.* **37** (1965) 71.
11. I. M. LIFSHITS and G. D. PARKHOMOVSKI, *Zh. Eksp. Theor. Fiz.* **20** (1950) 175.
12. A. B. BHATIA, *J. Acoust. Soc. Am.* **31** (1959) 16.
13. C. F. YING and R. TRUELL, *J. Appl. Phys.* **27** (1956) 1086.
14. G. JOHNSON and R. TRUELL, *ibid.* **36** (1971) 3466.
15. R. N. LATIFF and N. F. FIORE, *J. Acoust. Soc. Am.* **57** (1975) 1441.
16. E. P. PAPADAKIS, *ibid.* **37** (1965) 703.
17. A. G. EVANS, B. R. TITTMAN, L. AHLBERG, B. T. KHARI-YAKUB and G. S. KINO, *J. Appl. Phys.* **49** (1978) 12669.
18. D. K. MAK, *Br. J NDT* **33** (1991) 441.
19. E. R. GENERAGIO, *Rev. Progr. Quant. Non-Destruct. Eval.* **4B** (1985) 975.
20. E. E. UNDERWOOD, in "Quantitative Microscopy", edited by R. T. Dehoff and F. N. Rhines (McGraw–Hill, New York, 1968) p. 196.
21. J. H. POLARD, in "A Handbook of Numerical and Statistical Techniques" (Cambridge University Press, Cambridge, 1977) p. 122.

Received 15 June 1995
and accepted 12 August 1996